

Photon counting detector computed tomography in pediatric cardiothoracic CT imaging

Marilyn J. Siegel, MD^{1,*} and Juan C. Ramirez-Giraldo D PhD²

¹Edward Mallinckrodt Institute of Radiology, Washington University School of Medicine, St Louis, MO 63110, United States ²Siemens Healthineers, Computed Tomography, Malvern, PA 19355, United States

*Corresponding author: Marilyn J. Siegel, MD, Edward Mallinckrodt Institute of Radiology, Washington University School of Medicine, 510 S. Kingshighway Blvd., St Louis, MO 63110, United States (siegelm@wustl.edu)

Abstract

Photon-counting detector computed tomography (PCD-CT) is the most recent advancement in CT technology and has the potential to change clinical practice. Unlike conventional energy-integrated-detector (EID) that uses a two-step process to convert X-rays into a digital signal, PCD-CT directly converts photon energies into electronic signal. The advantages of PCD-CT over EID-CT are higher spatial resolution, electronic noise reduction, higher contrast-to-noise ratio, improved radiation dose efficiency, and intrinsic spectral imaging. Successful implementation into clinical practice requires adaptations in CT protocols. In this review, we summarize the basic principles of PCD-CT and technical scanning factors followed by a discussion of its clinical benefits in pediatric pulmonary and cardiovascular imaging.

Keywords: photon-counting computed tomography, pediatric imaging, CT imaging, cardiothoracic CT

Abbreviations

PCD-CT = photon-counting detector computed tomography, EID-CT = energy-integrating detector computed tomography, CNR = contrast-to-noise ratio, DECT = dual-energy CT, VNC = virtual non-contrast, VMI = virtual monoenergetic image, SR = standard resolution, UHR = ultra-high resolution, Sn = tin filtration, HRCT = high-resolution CT.

Summary

The technical advances of photon-counting detector CT, including improved spatial resolution and iodine signal, reduced electronic noise, and inherent spectral imaging, enhance visualization of small anatomic structures at reduced radiation dose.

Essentials

- The technical advances in PCD (photon-counting detector)-CT improve spatial resolution, contrast-to-noise ratio, and radiation dose efficiency.
- Inherent spectral reconstructions allow for improvement in image contrast and can play a role in lesion characterization and response assessment.
- The advantages of PCD-CT systems are especially important in pulmonary and cardiovascular imaging in children with small anatomic structures.
- · Protocol optimization is required to take advantage of the benefits of this imaging technology in clinical practice.

Introduction

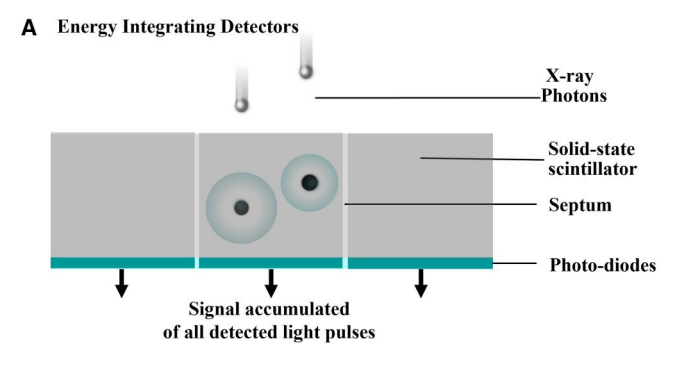
Photon-counting detector CT (PCD-CT) represents a major advancement in CT imaging technology, overcoming some of the technical limitations of current conventional energy-integrating detector computed tomography (EID-CT). ^{1–6} The result is improved visualization of small anatomic structures, potentially leading to improved anatomic precision at a lower radiation dose. ^{7–12} The unique technical features of PCD-CT technology have necessitated updated CT protocols for a range of diagnostic tasks. Early literature on the use of PCD-CT in the pediatric population has focused on lung, abdomen, and bone applications, showing promising clinical results. ^{7,13–16} Less is known about the potential of PCD-CT in pediatric cardiac and vascular imaging. ¹⁷ This article

reviews the basic principles of PCD-CT and technical scanning factors and discusses clinical benefits in pediatric lung, cardiac, and vascular imaging.

Basic principles

EID-CT technology

Current EID-CT uses solid-state scintillator crystals. The detectors absorb incident X-ray photons and convert them into visible light, and then in a second step, the light is detected by a photo-diode and converted into an electrical signal (Figure 1A). The accumulated output signal is "integrated" as the sum of all incoming photon energies to generate signal, thus the term "energy-integrated detector."



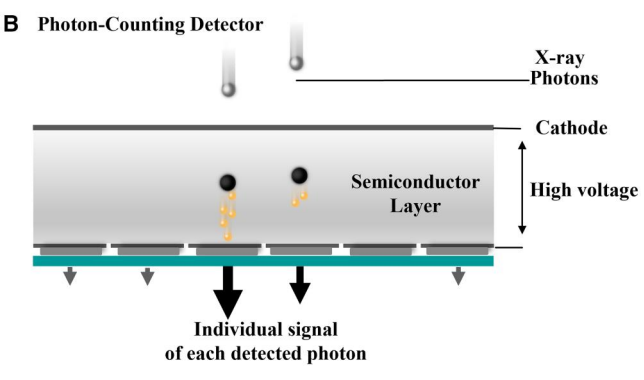


Figure 1. Detector configurations. (A) Energy integrating detectors. Incident X-rays are converted first to light at the scintillator layer and light is converted to an electrical signal by photo-diodes. Septa are required between pixels to avoid optical cross-talk, which reduces dose efficiency. (B) Photon-counting detector. Incident X-ray photons are directly converted into electrical signals. A high-voltage field causes X-ray photons to move from cathode to pixelated anodes producing current pulses which are converted into electrical pulses. Septa are not required. Arrows in both images = electrical signal output.

EID-CT scanners have some inherent limitations. First, septa are employed between detector elements to reduce "optical cross talk" (spread of visible light from one pixel to another pixel), reducing the effective detector area and spatial resolution. They create dead space where signal is not recorded, but X-ray photons are absorbed, limiting geometric dose efficiency. Second, due to output signal integration, lower energy photons, which are responsible for producing CT image contrast, are underweighted, resulting in decreased iodine signal and contrast-to-noise ratio (CNR). Third, electronic noise increases as doses are lowered. Fourth, EID-CT systems offer dual-energy CT (DECT) imaging, but with the exception of the dual-layer CT, the user has to define if the acquisition will be single energy or dual energy CT (DECT) prior to scan acquisition. ^{18,19}

PCD-CT technology

PCD-CT uses a semiconductor made of varying materials, including Cadmium Telluride, Cadmium Zinc Telluride, and Silicon. PCD-CT directly converts X-ray photons into electrical signals (Figure 1B). A high voltage applied across the semiconductor causes electrons to move towards pixelated anodes where they generate an electrical pulse. The energy of each detected electrical pulse is proportional to the photon's energy, and when the height of the pulse exceeds a predetermined threshold, it is counted in an energy bin, thus, the term "photon counting."

The PCD-CT detector has several advantages over EID-CT. First, the absence of reflective septa allows use of smaller detector elements compared to EID-CT (0.151 mm \times 0.176 mm vs. $0.45 \,\mathrm{mm} \times 0.51 \,\mathrm{mm}$ respectively), improving spatial resolution and dose efficiency. PCD-CT can also be operated with a larger matrix size (1024 \times 1024) compared to a typically smaller matrix size in EID-CT (512 \times 512). Second, by counting individual photons, greater weight is assigned to low energy photons, increasing iodine contrast-to-noise ratio and image quality. Third, in PCD-CT a preset kiloelectron threshold (20-25 keV) is applied to the pulse height analysis. This eliminates electronic noise, improving image quality at low radiation doses. 1-6 Finally, PCD-CT systems assign individual photons to multiple energy bins depending on the number of energy thresholds used. The system referred to in this article combines the information from four thresholds into two energy bins, low and high energy bins, which allows spectral imaging eg, virtual noncontrast (VNC) images, iodine maps, and low and high energy virtual monoenergetic images (VMI) reconstructions. Table 1 shows the technical features of PCD-CT and advantages of PCD-CT compared to EID-CT.

CT scan factors

The discussion below is based on our experience and clinical reports on NAEOTOM Alpha (Siemens Healthineers, Forchheim, Germany), which is a first-generation dual-source PCD-CT scanner with quantum technology. The technical factors specific to pulmonary and cardiothoracic scanning are provided in Table 2 and are based on our experience and reports from the literature.¹³

Image acquisition factors

Key acquisition parameters include resolution mode, tube potential (kilovoltage/kV), image quality reference level, pitch, and rotation time.

PCD-CT offers two different scan modes for data acquisition, which ultimately affect spatial resolution: standard resolution (SR) (144 \times 0.4 mm detector collimation) and ultrahigh resolution (UHR) mode (120 \times 0.2 mm collimation). Standard resolution mode has greater z-coverage (57.6 mm) allowing for faster scanning than UHR mode (z-coverage 24 mm). Because of the faster scan completion, contrast- and non-contrast and CT angiography scans are acquired with standard resolution mode. High-resolution lung CT is acquired with UHR mode to enable maximum spatial resolution.

PCD-CT images can be acquired at 70, 90, 120, and 140 kV and with 100 or 140 kV with tin filtration. The user selects the desired kV prior to scanning. In our practice, PCD-CT contrast-enhanced and non-enhanced chest and angiography studies are routinely acquired at 120 kV. Highresolution lung PCD-CT imaging is routinely performed using 100 kV with tin filtration (Sn100kV), which allows for lower radiation doses.^{20,21} Data are limited on imaging at low kV, but one article has shown that 90 kV imaging in congenital heart disease results in iodine contrast and image quality similar to that of EID-CT. 17 Imaging at low kV enables generation of virtual monoenergetic images, but iodine maps and virtual non-contrast images are not available. We prefer 120 kV over 70 or 90 kV imaging because it allows for generation of low keV images and the option for spectral capabilities.

Table 1. Advantages of technical features of photon-counting detector CT.

Feature	Advantage
Directly converts incident X-rays to signal	Output is proportional to individual photon energy
	Improves iodine signal as there is no down weighting of lower energy photons
Absence of reflective septae	Allows for smaller detector size which reduces radiation dose and improves
	spatial resolution
Use of energy-specific thresholding	Removes low-energy photons, eliminating electronic noise. Elimination of
	electronic noise improves image quality and allows imaging at lower
	radiation doses
Use of energy bins	Allows spectral imaging in every scan

Table 2. Acquisition and reconstruction scan factors for photon-counting detector CT examinations.

Examination	High-resolution lung	Contrast- and non-contrast chest	Angiography
Acquisition factors			
Resolution mode	Ultra-high resolution	Standard	Standard
Collimation [mm]	120×0.2	144×0.4	144×0.4
Tube potential [kV]	100 with tin filtration	120	120
Image quality level	38	29	35
Automated exposure control	Yes	Yes	Yes
Pitch	3.2	3.2	3.2
Rotation time (s)	0.25	0.25	0.25
Reconstruction factors			
Image format	Low threshold	70 kiloelectron volt (non-contrast CT) 60 kiloelectron volt (contrast CT)	55 kiloelectron volt
Kernel	Bl60 lung	Br40 soft tissue	Bv40 vessel
	0	B160 lung	B160 lung
Slice thickness (mm)	0.2, 1, 3	0.4, 1, 3	0.4, 1, 3
Matrix size	1024×1024	1024×1024	1024×1024
Quantum iterative reconstruction	3	3	3

Imaging at 140 kV also allows spectral reconstructions and it can reduce noise relative to lower tube potential values, but this comes at a higher radiation dose and reduction in contrast resolution, and thus is not routinely used in children.

All scans are performed with automated exposure control and an algorithm that selects an image quality (IQ) level, ranging between 29 and 38 for cardiothoracic imaging, to optimize tube current settings and select the virtual monoenergetic image (VMI) level and required dose for the examination. All scans are acquired with high-pitch mode of 3.2 and fast rotation time (0.25 s).

Image reconstruction factors

Reconstruction parameters include image format, kernel, slice thickness, matrix size, and iterative reconstruction algorithm.

PCD-CT enables two image formats: VMI and low threshold energy reconstructions. VMIs are the default for contrast-and non-contrast and CT angiography scans and are based on the diagnostic task: 55 keV for angiography, 60 keV for contrast chest, and 70 keV for non-contrast examinations (Figure 2). The low threshold energy reconstruction has characteristics comparable to standard EID-CT polychromatic images and is the default for UHR scanning. Reconstruction kernels are dependent on the diagnostic task: Br40 for soft tissues, Bl60 for lung, and Bv60 for vessels. Upper case "B" specifies body imaging, lower case letters specify a specific anatomic area ("r", regular/soft tissue, "v", vascular, "l", lung) and numbers specify image sharpness, with higher numbers having sharper resolution (Figure 3). Reconstruction slice thicknesses are 0.2 for UHR and 0.4 mm for standard

resolution scans, representing the thinnest available slice thicknesses for each mode. Both UHR and standard resolution scans are also reconstructed with thicker slices (1 and 3 mm). Matrix size for all scans is 1024×1024 . All image sets are reconstructed using quantum iterative reconstruction (QIR) at a level of 3, based on published reconstruction algorithms. $^{3,7,13-15,22}$ Higher keV images and iterative metal artifact reduction (iMAR) software are available to reduce metal artifacts. 22,23 Window levels and widths are the same that are used in EID-CT.

Safety issues

Radiation dose reduction

Radiation exposure from CT is an important consideration in children because of concerns about the potential risk for radiation-induced carcinogenesis. PCD-CT increases dose efficiency by eliminating reflective septa between detector elements and electronic noise (see discussion above on PCD-CT Technology). Additionally, PCD-CT uses tin filtration for UHR scanning removing low-energy photons that do not substantially contribute to image quality but do contribute to the radiation burden. The system also uses technologies which have been the cornerstones of CT dose optimization, including automated exposure control and automated kilovoltage selection.

Contrast media dose reduction

PCDs count each individual photon regardless of its energy, allowing low-energy photons which have more iodine signal than high-energy photons, to have more weighting in the



Figure 2. Contrast-enhanced chest CT in 3-year-old girl. Low kiloelectron voltage (keV) reconstructions at (A) 55 keV, (B) 60 keV and (C) 70 keV. Image acquired with 0.4 mm collimation, 120 kV, pitch 3.2, and reconstructed at 1-mm slice thickness. Iodine contrast reported in Hounsfield units (HU) increases with lower keV. In this example, mean CT numbers in the descending aorta are 390 HU at 55 keV, 325 HU at 60 keV, and 220 HU at 70 keV. Images are displayed with identical soft tissue window level settings: width = 400 HU, level = 40 HU.

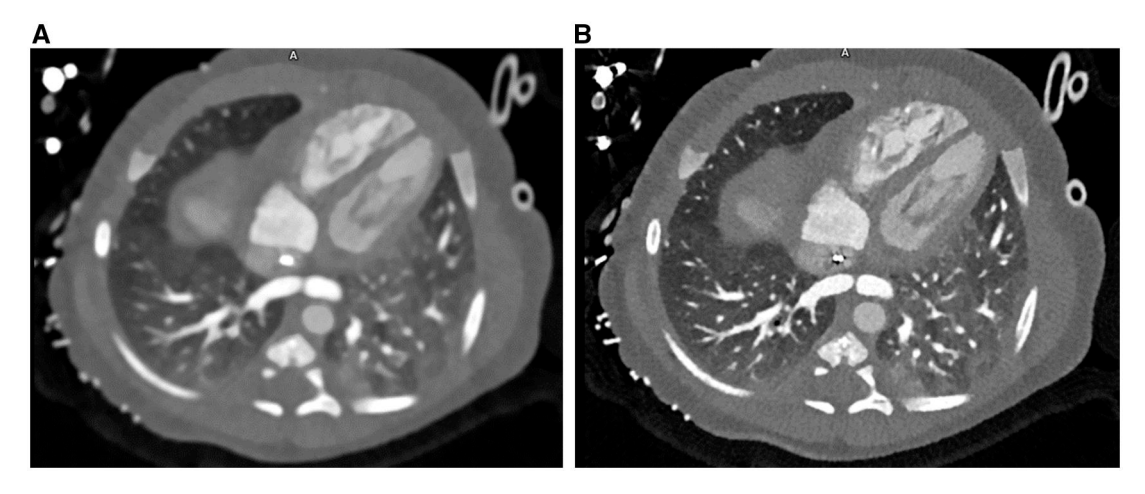


Figure 3. Three-day-old girl. CT angiography performed for evaluation of a possible vascular ring. PCD-CT image acquired with 0.4 mm collimation, 120 kV, pitch 3.2, and reconstructed at 1-mm slice thickness at 55 keV. Images are shown with (A) Soft-tissue kernel (Br40) and (B) lung kernel (Bl60). Soft tissue kernels reduce image noise and facilitate evaluation of low-contrast features but blur details, while sharper kernels, such as lung, enable visualization of smaller structures, albeit at the cost of increased image noise.

signal output than they have in EID-CT, thus increasing iodine signal-to-noise ratio. In addition, PCD-CT uses threshold binning of the electrical signals, which allows generation of virtual monoenergetic images at lower photon energies (eg, 55-60 keV) in contrast-enhanced scans, thereby increasing iodine signal.

Higher iodine signal can translate into reduced volumes of intravenous contrast agent required for CT examinations. Higashigaito et al, in a study of aortic angiography in adults, showed that a 25% reduction in contrast media volume with VMI reconstructions at 50 keV yielded non-inferior image quality compared to EID-CT.²⁴ In a pediatric study, Cao et al suggested that reduced contrast volume was also feasible in PCD-CT, especially when combined with low-energy VMI reconstructions.⁷

The use of low-volume contrast media protocols can be advantageous in patients with impaired renal function and in very young children, with small-gauge intravenous catheters in whom venous access may be limited.

Clinical benefits: thorax Parenchymal lung disease

Non-contrast, high-resolution CT (HRCT) has become the standard imaging technique for evaluating lung parenchyma and surrounding structures. Recent experience with PCD-CT

has shown that it has potential to improve imaging of fine structures in the lung parenchyma secondary to the use of thinner slices compared to EID-CT (0.2 and 0.4 mm vs. $0.6 \,\mathrm{mm}$, respectively) and larger matrix sizes (1024 × 1024 vs. 512×512 , respectively). 25-27

Bartlett et al compared lung PCD-CT and high-resolution EID-CT images and reported improved detection of higher-order bronchi and bronchial walls.²⁵ In the same study, the authors suggested that PCD-CT offered benefits in visualization of pathologies, such as honeycombing, fibrosis, and emphysema compared with routine clinical scans. Inoue et al reported that PCD-CT increased reader confidence for the presence or absence of reticulation, ground-glass opacity, and mosaic attenuation pattern compared to EID-CT, which in turn increased accuracy in the diagnosis of usual interstitial pneumonia.²⁷

Our personal experience supports that the increased spatial resolution of PCD-CT increases visualization of small lung structures compared with EID-CT, which enables better characterization of morphology in a pediatric population. Figures 4 and 5 show better visualization of bronchi, fissures, and mosaic attenuation on UHR PCD-CT in children with airway diseases.

In addition, several studies have reported that high-resolution PCD-CT enables a greater dose reduction compared to EID-CT. ^{28,29} Jungblut et al, in a study imaging

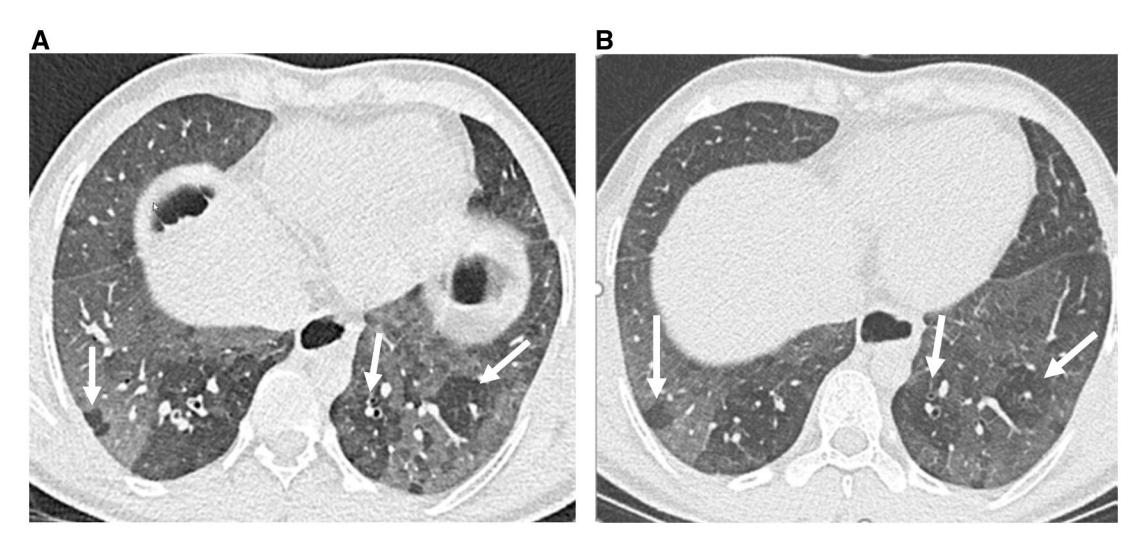


Figure 4. Sixteen-year-old girl. CT performed for routine follow-up for bronchiolitis obliterans following lung transplant in infancy. (A) Ultra-high resolution PCD-CT image acquired with 0.2 mm collimation, Sn100 kV, pitch 3.2, low threshold reconstruction; CTDI_{vol} 0.64 mGy. (B) High-resolution EID-CT scan 12 months earlier at 0.6 mm collimation, Sn100 kV, pitch 1.55 (standard on EID-CT); CTDI_{vol} 1.08 mGy. Low attenuation areas characteristic of mosaic attenuation pattern (arrows) are more conspicuous on PCD-CT than on EID-CT related to improved spatial resolution.

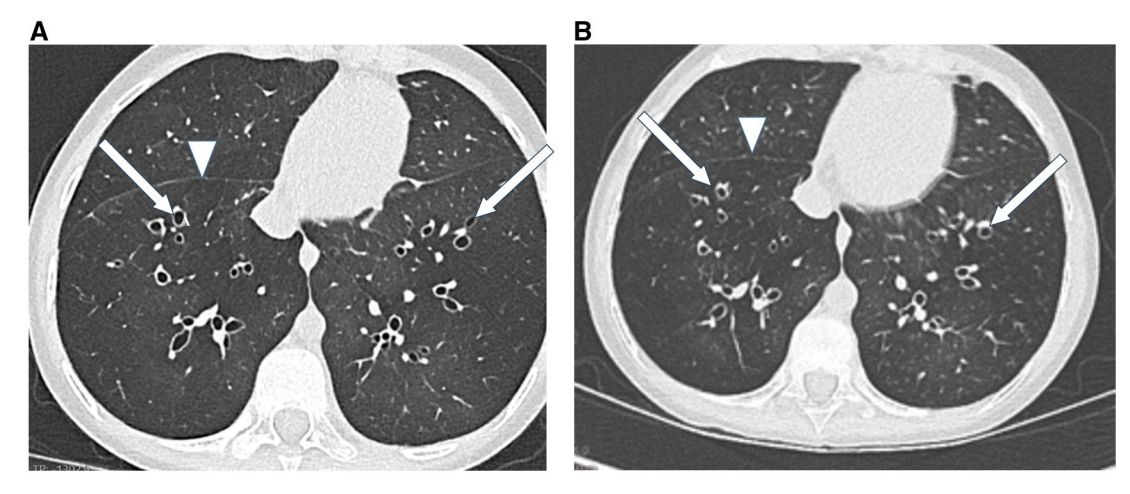


Figure 5. Six-year-old girl. CT performed for follow-up of cystic fibrosis. (A) Ultra-high resolution PCD-CT image acquired with 0.2 mm collimation, Sn100 kV, pitch 3.2, low threshold reconstruction; CTDI_{vol} 0.39 mGy. (B) High-resolution EID-CT scan 6 months earlier at 0.6 mm collimation, Sn100 kV, pitch 1.55; CTDI_{vol} 0.74 mGy. PCD-CT improves definition of bronchial walls (arrows) and lung fissures (arrowhead) and reduces radiation exposure.

adults with systemic sclerosis, showed a 66% dose reduction using UHR PCD-CT with diagnostic accuracy similar to third-generation EID-CT. 29 Graffen et al reported a 50% dose reduction on PCD-CT compared to EID-CT with similar or better objective and subjective image quality. 28 In a pediatric study, Horst et al showed that the UHR mode enabled diagnostic image quality for assessing cystic fibrosis Brody II score at radiation doses (CT dose index volume/CTDI_{vol} mean 0.07 \pm 0.03 mGy) similar to those of conventional chest radiographs. 14 Siegel et al reported a 42% dose reduction on PCD-CT compared to EID-CT in an age-matched pediatric population (CTDI_{vol} 0.41 mGy vs. 0.71 mGy). 15 Subjective image analysis showed no differences in image quality. 15

Lung nodules

PCD-CT also has the potential to improve lung nodule characterization, such as matrix (ground-glass, subsolid, or solid), edges (regular or irregular), and size, related to the use of thinner slices compared to EID-CT (0.2 and 0.4 mm vs. 0.6 mm, respectively) and larger matrix sizes. In a phantom study evaluating morphology of synthetic lung nodules,

Zhou et al reported that UHR mode of PCD-CT improved nodule shape characterization and accuracy for measuring nodule volume compared with conventional EID-CT scans. In a pediatric population, Cao et al suggested that the improved edge definition of pulmonary nodules and adjacent structures afforded by PCD-CT may impact management such as decision to perform metastasectomy. Figure 6 illustrates the improved definition of nodule edges and shape on PCD-CT compared to EID-CT.

Mediastinum

Standard resolution, contrast-enhanced chest CT is the preferred screening study for evaluation of mediastinal masses. In an adult oncologic cohort, Hagen et al compared doses and image quality, based on analysis of CNR in vessels, lung, chest muscle, and subcutaneous fat, on contrast-enhanced UHR PCD-CT compared to EID-CT. Their results showed that PCD-CT enabled significant reduction in CTDI_{vol} from 7.21 ± 0.49 mGy for EID-CT to 4.17 ± 1.29 mGy for PCD-CT (43% reduction, P < .001) while yielding similar image quality. In a pediatric study with matched patient cohorts

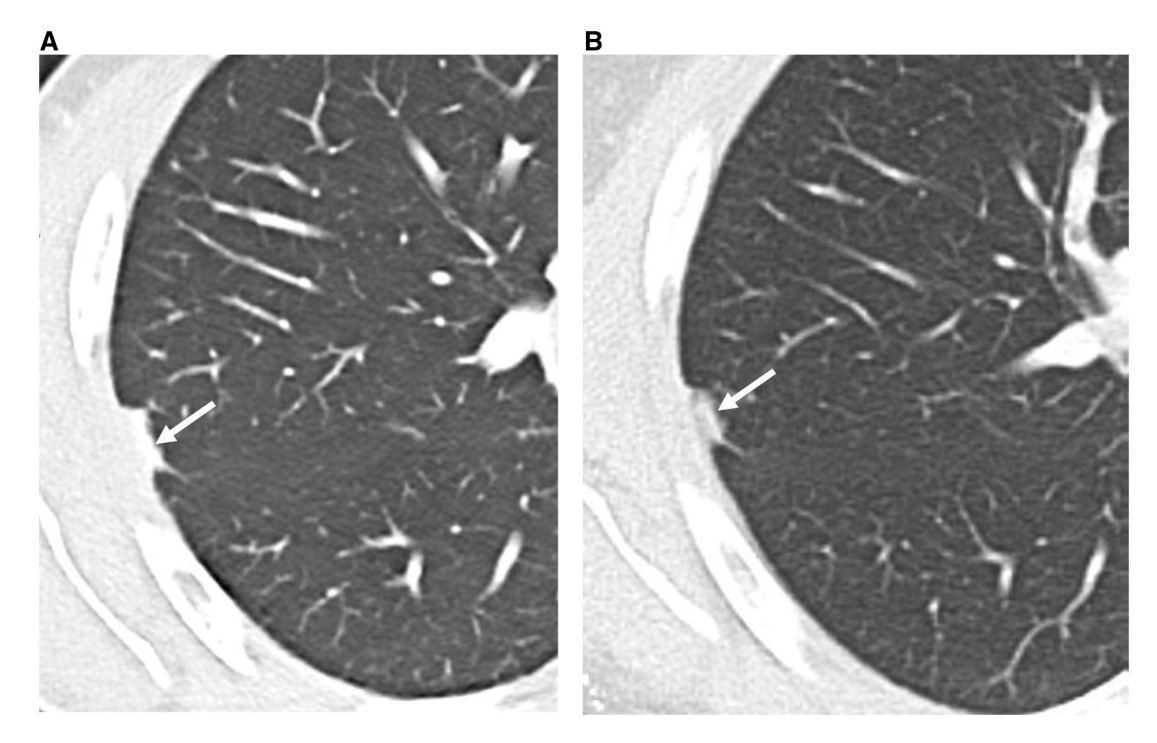


Figure 6. Seventeen-year-old boy with metastatic testicular germ cell tumor. Contrast-enhanced chest and abdomen CT for tumor surveillance. (A) PCD-CT image acquired with 0.4 mm collimation, 120 kV, pitch 3.2, 60 keV reconstruction; CTDI_{vol} 4.5 mGy. (B) EID-CT scan 6 months earlier at 0.6 mm collimation, 100 kV, pitch 3.2; CTDI_{vol} 5.7 mGy. Right middle lung nodule is present in both images (arrows). Lesion edges as well as adjacent parenchymal vessels are better defined on PCD-CT than EID-CT at reduced radiation dose.

comparing radiation dose on contrast-enhanced chest PCD-CT at $120\,\mathrm{kV}$ and EID-CT at 70 or $80\,\mathrm{kV}$, the authors reported 65% dose reduction (mean CTDI_{vol} 1.4 mGy PCD-CT vs. $4.0\,\mathrm{mGy}$ EID-CT). Image quality was diagnostic for all studies.

Clinical benefits: cardiovascular applications

The discussion of cardiovascular imaging will focus on use of non-electrocardiogram-gated (ECG), high-pitch PCD-CT for evaluation of congenital heart lesions, extracardiac vessel anomalies, and patency of stents. ECG-gated-CT is not a common examination and is reserved for evaluation of coronary artery anomalies, which are rare in the pediatric population.

Congenital heart disease

In an evaluation of congenital heart defects in a pediatric cohort, Dirichs et al showed that PCD-CT acquired at 90 kV offered higher contrast-to-noise ratios compared to EID-CT at 70 kV (62.0 ± 50.3 vs. 37.2 ± 20.8 , respectively, P = .001) with equivalent radiation doses.¹⁷

In our experience, we have found that non-ECG-gated PCD-CT acquired at 120 kV with 0.4 mm collimation improves subjective cardiac imaging quality in children undergoing evaluation of congenital heart disease compared to EID-CT with lower radiation doses. PCD-CT provides a clearer depiction of normal anatomic structures, such as the ventricular walls and papillary muscles, and intracardiac pathology. Figure 7 shows better margin definition and contrast enhancement in intra-cardiac shunt lesions on PCD-CT compared to EID-CT. The advantage of 120 kV scanning is that it enables low-energy and material specific images, which can be useful to improve iodine signal and assess pulmonary

blood flow, respectively (see section below on spectral imaging).

Although non-gated PCD-CT is not routinely performed for coronary artery evaluation, the proximal segments of the coronary arteries are often seen on non-gated CT acquired for evaluation of congenital heart disease, likely reflecting the high spatial resolution of this technology. This capability has the potential to eliminate further imaging with a dedicated ECG-CT examination. Figure 8 shows that the higher resolution of PCD-CT allows for a better definition of origins and proximal branches of the coronary arteries compared to EID-CT.

Stents

CT evaluation of metal stents can be hampered by blooming, beam-hardening, and motion artifacts related to high heart rates. Due to these artifacts, stent diameters can appear larger than they actually are and visualization of the stent lumen can be limited. Adult publications have shown that UHR PCD-CT can overcome these limitations because of its increased spatial resolution and noise reduction, allowing for more accurate measurement of stent diameters and stenosis, which in turn can impact optimal medical or surgical management. 33

Indications for stents in children are treatment of obstructive lesions involving the pulmonary artery, aorta, and systemic or pulmonary veins and maintenance of patency of ductus-dependent circulation, aortopulmonary collateral vessels, and surgical shunts. In our experience, PCD-CT has the potential to improve definition of stent walls and reduce intraluminal artifacts, allowing for better evaluation of stent diameters and luminal patency and assessment for stenosis. Figure 9 illustrates better delineation of stent walls and

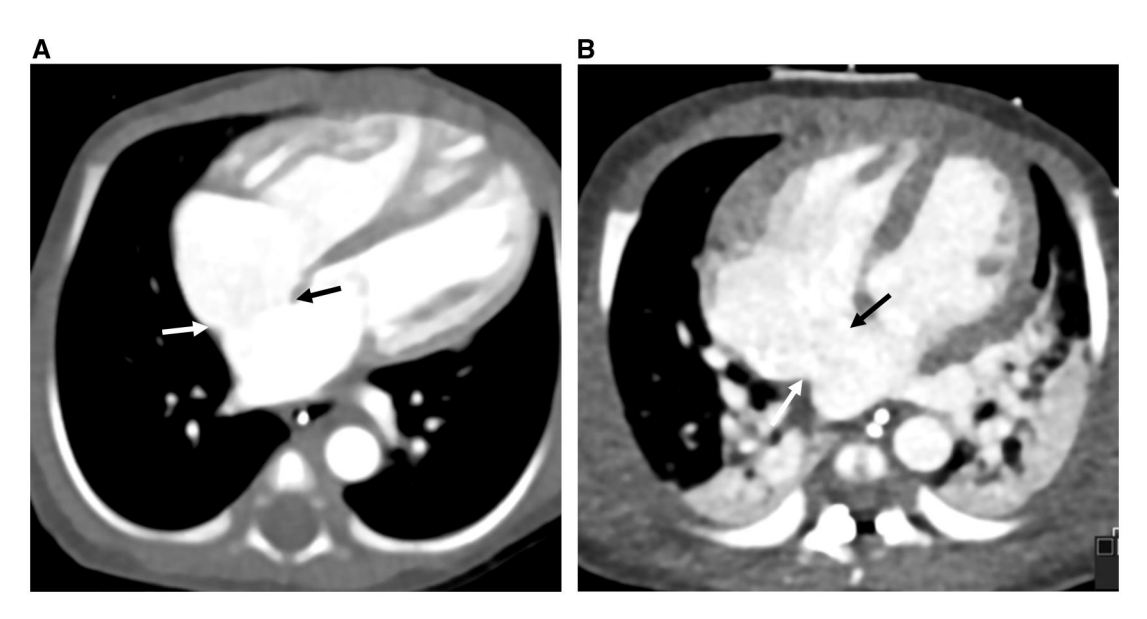


Figure 7. CT angiography for evaluation of congenital heart disease. Secundum atrial septal defects in two neonates. (A) PCD-CT image acquired at 0.4 mm collimation, 120 kV, pitch 3.255 keV reconstruction; CTDI_{vol} 0.45 mGy. (B) EID-CT image acquired at 0.6 mm collimation, 70 kV, pitch 3.2; CTDI_{vol} 0.47 mGy. PCD-CT more clearly depicts edges of the septal defect (arrows) and results in increased iodine contrast enhancement, which can allow for more reliable measurements. Ventricular walls and left papillary muscles are also better defined.

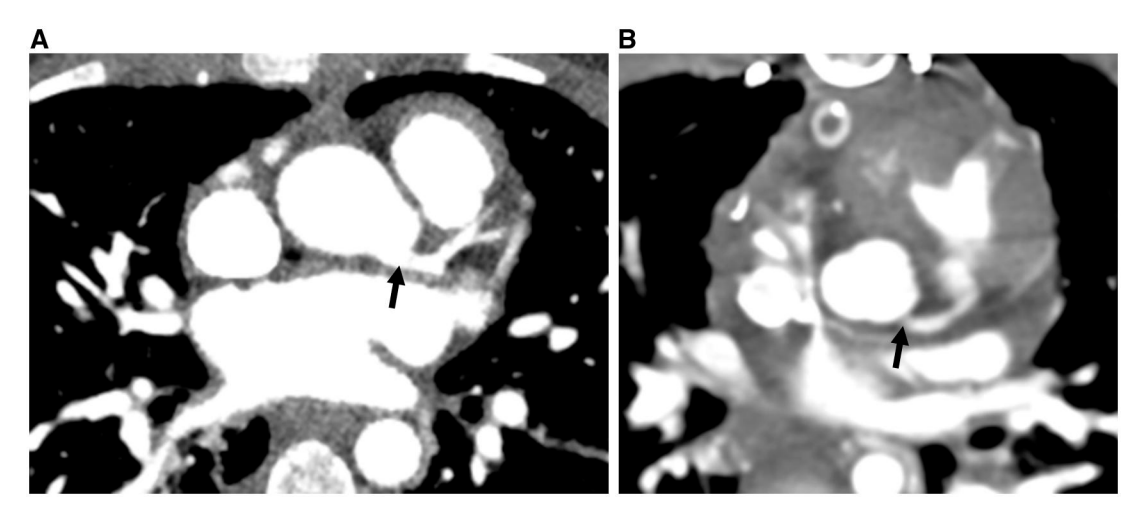


Figure 8. CT for evaluation of congenital heart disease. (A) Seven-year-old boy. PCD-CT image acquired at 0.4 mm collimation, 120 kV, pitch 3.2, 55 keV reconstruction; CTDI_{vol} 0.84 mGy. (B) Five-year-old boy. EID-CT image acquired at 0.6 mm collimation, 70 kV, pitch 3.2; CTDI_{vol} 0.94 mGy. Delineation of origin (arrows) and proximal segments of the coronary arteries are improved on PCD-CT.

luminal diameter on PCD-CT compared to EID-CT and also shows improved dose efficiency.

Thoracic vessels

The higher spatial resolution of PCD-CT also has advantages in evaluation of the extracardiac arteries, veins, and their branches. In pediatric practice, high spatial resolution images and high iodine signal are critical in characterizing small vascular pathologies, such as aortic coarctation, patent ductus arteriosus, pulmonary embolus, and pulmonary branch vessel stenosis, allowing for better edge and size definition compared with EID-CT. Figure 10 shows the advantage of high spatial resolution obtained using PCD-CT compared with EID-CT to assess congenital vascular anomalies.

Studies in adults have shown that use of low-energy VMIs can impact visualization of contrast enhancement in thoracic

vessels. In aortic imaging, Euler et al showed that PCD-CT acquired at 120 kV and 0.4 mm with low-energy VMIs levels (40 to 45 keV) resulted in significantly increased CNR (up to 34% difference) compared to EID-CT at matched radiation dose.³⁴ We have found that 55 keV offers the optimal subjective contrast visualization and lowest noise in pediatric CT angiography of the thoracic arteries. While we recognize that VMI energy levels at 40 or 45 keV will increase contrast more than those at 55 keV images, they come with the penalty of more noise in children than in adults related to the routine use of lower radiation doses in children than in adults. In addition to allowing a high iodine signal, PCD-CT angiography reduces radiation dose. One study comparing thoracic angiography in children on PCD-CT and EID-CT, reported a 50% dose reduction (mean CTDIvol 1.9 mGy vs. 3.9 mGy respectively) with the use of PCD-CT.³²

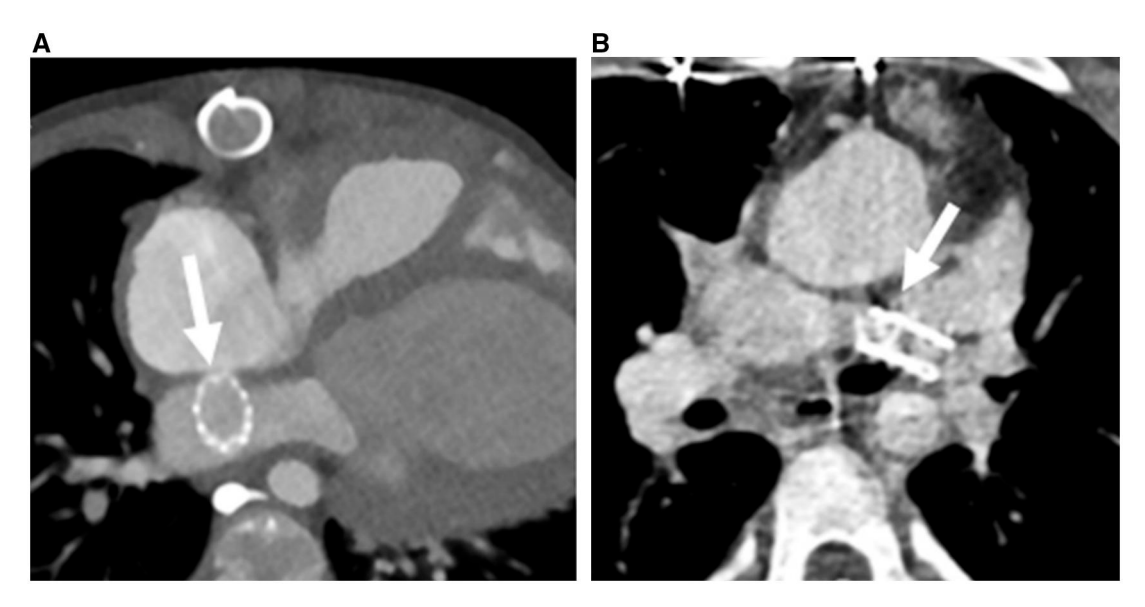


Figure 9. CT angiography in two different patients undergoing follow-up examination for stent evaluation. (A) Three-year-old boy with pulmonary artery atresia and stent in a patent foramen oval (arrow). PCD-CT image acquired at 0.4 mm collimation, 120 kV, pitch 3.2, 55 keV reconstruction; CTDI_{vol} 0.67 mGy. (B) Five-year-old boy with pulmonary atresia and stented left pulmonary artery (arrow). EID-CT image acquired at 0.6 mm collimation, 70 kV, pitch 3.2; CTDI_{vol} 1.02 mGy. PCD-CT eliminates blooming artifacts, improving definition of stent walls and vessel lumen, allowing a better evaluation of stent patency and diameter at a dose reduction.

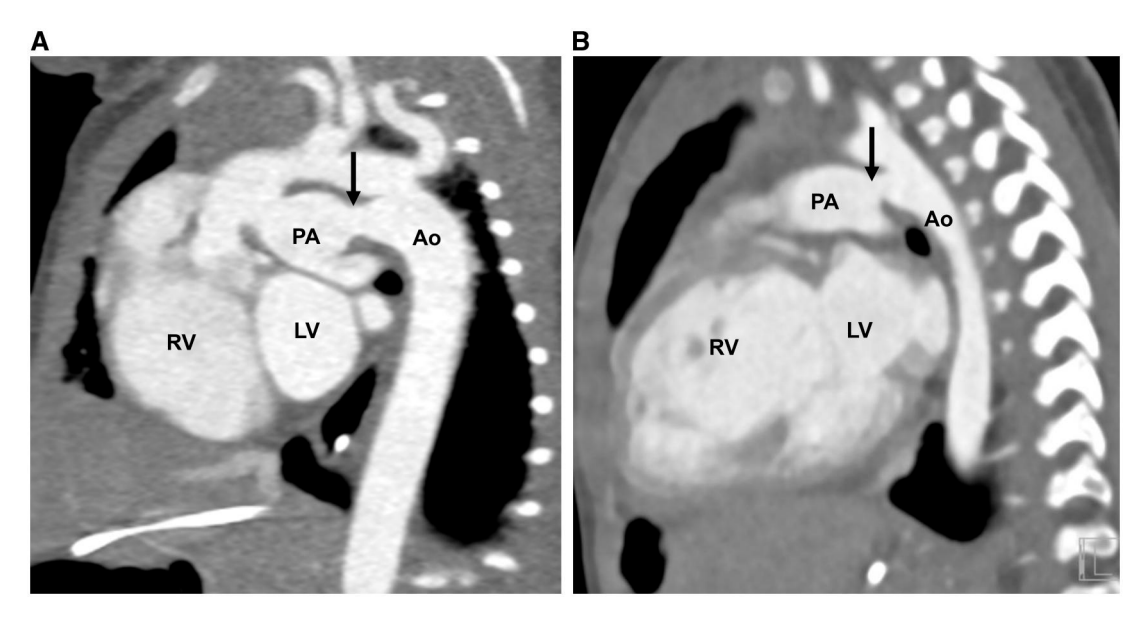


Figure 10. Patent ductus arteriosus. (A) One-month-old infant. PCD-CT image acquired at 0.4 collimation, 120 kV, pitch 3.2; 55 keV reconstruction; CTDI_{vol} 0.75 mGy. (B) Two-month-old infant. EID-CT image acquired at 0.6 mm collimation, 70 kV, pitch 3.2; CTDI_{vol} 0.91 mGy. Higher spatial resolution of PCD-CT improves definition of margins of patent ductus arteriosus (arrows) between aorta (Ao) and pulmonary artery (PA) and ventricular walls at lower radiation doses. RV = right ventricle. LV = left ventricle.

Simultaneous spectral imaging

Spectral, also termed multienergy, CT refers to the use of two or more photon spectra to create images. A unique feature of PCD-CT is its ability to provide spectral information in every scan using a single tube potential (120 kV) owing to its ability to detect energy of individual photons.

VMIs are routinely constructed at different energies depending on the diagnostic task. Low-energy keV (55 keV) VMIs are useful to increase the conspicuity of iodinated contrast material, while higher keV (60 and 70 keV) VMIs are useful to decrease noise levels. As noted earlier, typical energy levels for common diagnostic tasks are 55 keV for angiography, 60 keV for

contrast-enhanced soft tissue, 65 keV for bone, and 70 keV for non-contrast CT.

Spectral imaging also enables generation of material-specific images, including iodine maps and virtual non-contrast images. Iodine maps can play a role in assessing the presence of contrast material in mediastinal and chest wall masses, lung nodules, and adenopathy, which can help in lesion characterization and treatment response assessment. ^{18,19,35} They also can play a role in assessing lung perfusion. Figures 11 and 12 illustrate the benefits of iodine mapping in mediastinal and vascular imaging. Similarly, virtual non-contrast images can be useful to determine whether high-attenuating lesions seen on contrast-enhanced CT

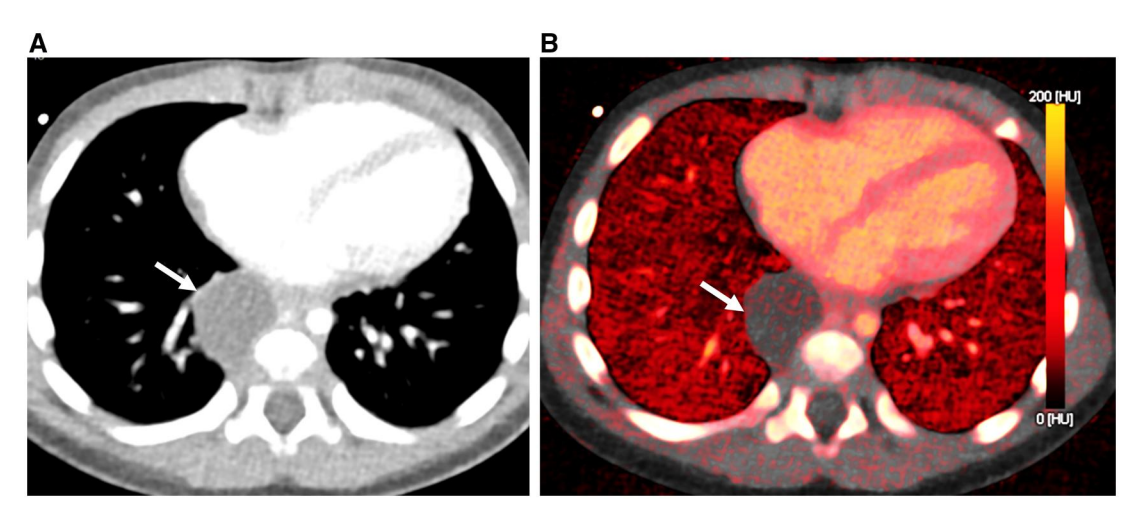


Figure 11. Eleven-month-old boy with cough. Chest CT performed to evaluate a mass detected on chest X-ray. (A) PCD-CT image acquired at 0.4 mm collimation, 120 kV, pitch 3.2, 60 keV reconstruction shows a low attenuation mass (arrows) with mean attenuation of 35 Hounsfield Units. (B) lodine map demonstrates absent iodine content, increasing confidence in diagnosis of a benign cystic mass. Foregut duplication cyst proven at surgery. One of the advantages of PCD-CT over EID-CT is the capability to perform spectral imaging in every scan.

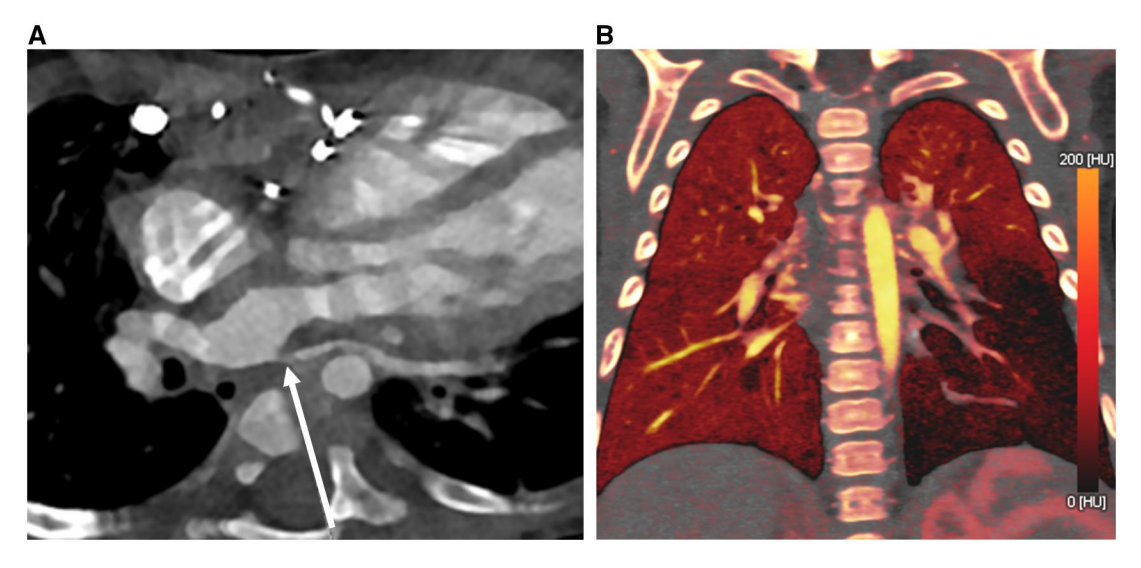


Figure 12. Ten-month-old boy post-transplant for hypoplastic left heart syndrome. (A) Chest CT angiography acquired at 0.4 mm collimation, 120 kV, pitch 3.2, and 55 keV reconstruction demonstrates severe stenosis at the left inferior pulmonary vein (arrow). (B) Iodine map demonstrates reduced iodine content in the left lower lung, indicating reduced blood flow due to increased capillary pressure and pulmonary congestion.

images represent iodine enhancement or other materials, such as calcium or blood products.

At the time of submitting this article, FDA approval is pending in the United States for additional material-specific applications that include lung-perfused blood volume (PBV) and lung vessel analysis. These spectral applications can have a role in evaluating perfusion in vascular and parenchymal diseases.

Summary

PCD-CT offers promise in overcoming limitations of EID-CT in clinical practice in children. The advantages over EID-CT, including superior spatial resolution, iodine contrast and noise properties, and intrinsic spectral imaging, can improve visualization of small physiologic and pathological structures and increase diagnostic confidence in lung and cardiovascular imaging tasks in children. PCD-CT can also have a role in radiation dose reduction, which is of high importance in

imaging children. To successfully harness these benefits, it is crucial to select specific scanning factors that take advantage of PCD technology. This article hopefully will facilitate adoption of this technology into lung and cardiovascular imaging in children. Although early experience is encouraging, there is a need for future studies assessing the capabilities of PCD-CT in larger patient cohorts and its effect on diagnostic sensitivity and classification of lung and cardiovascular diseases. Additional future research needs to assess impact of deep learning in image reconstruction and noise reduction algorithms^{8,9} on PCD-CT image quality, radiation dose, and improved diagnostic accuracy.

Author contributions

Marilyn J. Siegel (Conceptualization, Formal Analysis, Investigation, Methodology, Project Administration, Supervision, Writing-original draft, Writing-review &

editing). Juan C Ramirez-Giraldo (Conceptualization, Formal Analysis, Investigation, Methodology, Writing-original draft, Writing-review & editing).

Supplementary material

Supplementary material is available at Radiology Advances online.

Funding

No funding was received for conducting this study.

Conflicts of interest

Please see ICMJE form(s) for author conflicts of interest. These have been provided as supplementary materials. M.J.S. has received lecture honoraria in the past for Siemens Healthineers. J.C.R.G. is a scientist employed by Siemens Healthineers. The author who is not an employee of the industry had full control of the data and information submitted for publication.

References

- 1. Esquivel A, Ferrero A, Mileto A, et al. Photon-counting detector CT: key points radiologists should know. *Korean J Radiol.* 2022; 23(9):854-865. https://doi.org/10.3348/kjr.2022.0377
- Flohr T, Schmidt B. Technical basics and clinical benefits of photon-counting CT. *Invest Radiol*. 2023;58(7):441-450. https:// doi.org/10.1097/RLI.0000000000000980
- Leng S, Bruesewitz M, Tao S, et al. Photon-counting detector CT: system design and clinical applications of an emerging technology. *Radiographics*. 2019;39(3):729-743. https://doi.org/10.1148/rg. 2019180115
- McCollough CH, Rajendran K, Leng S, et al. The technical development of photon-counting detector CT. Eur Radiol. 2023;33(8): 5321-5330. https://doi.org/10.1007/s00330-023-09545-9
- Rajendran K, Petersilka M, Henning A, et al. First clinical photoncounting detector CT system: technical evaluation. *Radiology*. 2022;303(1):130-138. https://doi.org/10.1148/radiol.212579
- Willemink MJ, Persson M, Pourmorteza A, et al. Photon-counting CT: technical principles and clinical prospects. *Radiology*. 2018; 289(2):293-312. https://doi.org/10.1148/radiol.2018172656.
- Cao J, Bache S, Schwartz FR, Frush D. Pediatric applications of photon-counting detector CT. AJR Am J Roentgenol. 2023;220 (4):580-589. https://doi.org/10.2214/AJR.22.28391
- 8. Fletcher JG, Inoue A, Bratt A, et al. Photon-counting CT in thoracic imaging: early clinical evidence and incorporation into clinical practice. *Radiology*. 2024;310(3):e231986. https://doi.org/10.1148/radiol.231986
- McCollough CH, Rajendran K, Baffour FI, et al. Clinical applications of photon counting detector CT. Eur Radiol. 2023;33(8): 5309-5320. https://doi.org/10.1007/s00330-023-09596-y.
- Nehra AK, Rajendran K, Baffour FI, et al. Seeing more with less: clinical benefits of photon-counting detector CT. *Radiographics*. 2023;43(5):e220158. https://doi.org/10.1148/rg.220158
- 11. Tortora M, Gemini L, D"Iglio I, et al. Spectral photon-counting computed tomography: a review on technical principles and clinical applications. *J Imaging*. 2022;8(4):112. https://doi.org/10.3390/jimaging8040112.
- 12. van der Bie J, van Straten M, Booij R, et al. Photon-counting CT: review of initial clinical results. *Eur J Radiol.* 2023;163:110829. https://doi.org/10.1016/j.ejrad.2023.110829
- 13. Horst KK, Yu L, McCollough CH, et al. Potential benefits of photon counting detector computed tomography in pediatric imaging.

- *Br J Radiol.* 2023;96(1152):20230189. https://doi.org/10.1259/bir.20230189.
- Horst KK, Hull NC, Thacker PG, et al. Pilot study to determine whether reduced-dose photon-counting detector chest computed tomography can reliably display Brody II score imaging findings for children with cystic fibrosis at radiation doses that approximate radiographs. *Pediatr Radiol.* 2023;53(6):1049-1056. https:// doi.org/10.1007/s00247-022-05574-6
- Siegel MJ, Bugenhagen S, Sanchez A, et al. Comparison of photoncounting detector CT with energy-integrated detector CT on radiation dose and image quality in pediatric high-resolution chest CT. AJR Am J Roentgenol. 2023;221(3):363-371. https://doi.org/10. 2214/AJR.23.29077
- Tsiflikas I, Thater G, Ayx I, et al. Low dose pediatric chest computed tomography on a photon counting detector system-initial clinical experience. *Pediatr Radiol*. 2023;53(6):1057-1062. https://doi.org/10.1007/s00247-022-05584-4
- Dirrichs T, Tietz E, Ruffer A, et al. Photon-counting versus dualsource CT of congenital heart defects in neonates and infants; initial experience. *Radiology*. 2023;307(5):e223088. https://doi.org/ 10.1148/radiol.223088
- Rapp JB, Biko KM, Siegel MJ. Dual-energy CT for pediatric thoracic imaging: a review. AJR Am J Roentgenol. 2023;221(4): 526-538. https://doi.org/10.2214/AJR.23.29244
- Siegel MJ, Ramirez-Giraldo JC. Dual-energy CT in children: imaging algorithms and clinical applications. *Radiology*. 2019;291(2): 286-297. https://doi.org/10.1148/radiol.2019182289
- Bodelle B, Fischbach C, Booz C, et al. Single-energy pediatric chest computed tomography with spectral filtration at 100 kVp: effects on radiation parameters and image quality. *Pediatr Radiol*. 2017; 47(7):831-837. https://doi.org/10.1007/s00247-017-3813-1
- Siegel MJ, Raptis D, Bhalla S, Ramirez-Giraldo JC. Comparison of 100-kilovoltage tin filtration with advanced modeled iterative reconstruction on radiation dose and image quality in pediatric nonncontrast-enhanced chest computed tomography. *J Comput Assist Tomogr.* 2022;46(1):64-70. https://doi.org/10.1097/RCT. 00000000000001248.
- 22. Sartoretti T, Racine D, Mergen V, et al. Quantum iterative reconstruction for low dose ultrahigh resolution photon counting detector CT of the lung. *Diagnostics (Basel)*. 2022;12(2):522. https://doi.org/10.3390/diagnostics12020522.
- Anhaus JA, Killermann P, Mahnken AH, Hoffmann C. A nonlinear scaling-based normalized metal artifact reduction to reduce low-frequency artifacts in energy-integrating and photon-counting CT. *Med Phys.* 2023;50(8):4721-4733. https://doi.org/10.1002/mp.16461
- Higashigaito K, Mergen V, Eberhard M, et al. CT angiography of the aorta using photon-counting detector CT with reduced contrast media volume. *Radiol Cardiothorac Imaging*. 2023;5(1): e220140. https://doi.org/10.1148/ryct.220140
- Bartlett DJ, Wan KC, Bartholmai B, et al. High-resolution chest computed tomography imaging of the lungs: impact of 1024 matrix reconstruction and photon-counting detector computed tomography. *Invest Radiol*. 2019;54(3):129-137. https://doi.org/10. 1097/RLI.0000000000000524
- Si-Mohamed S, Boccalini S, Rodesch P-A, et al. Feasibility of lung imaging with a large field-of-view spectral photon counting CT system. *Diagn Interv Imaging*. 2021;102(5):305-312. https://doi. org/10.1016/j.diii.2021.01.001
- 27. Inoue A, Johnson TF, White D, et al. Estimating the clinical impact of photon-counting-detector CT in diagnosing usual interstitial pneumonia. *Invest Radiol.* 2022;57(11):734-741. https://doi.org/10.1097/rli.0000000000000888
- Graafen D, Emrich T, Halfmann MC, et al. Dose reduction and image quality in photon-counting detector high-resolution computed tomography of the chest. Routine clinical data. *J Thorac Imaging*. 2022;37(5):315-322. https://doi.org/10.1097/RTI.0000 0000000000661
- 29. Jungblut L, Euler A, Spiczak J, et al. Potential of photon-counting detector CT for radiation dose reduction for the assessment of

- interstitial lung disease in patients with systemic sclerosis. *Invest Radiol*. 2022;57(12):773-779. https://doi.org/10.1097/RLI.0000
- Zhou W, Montoya J, Gutjahr R, et al. Lung nodule volume quantification and shape differentiation with an ultra-high resolution technique on a photon-counting detector computed tomography system. *J Med Imaging (Bellingham)*. 2017;4(4):043502. https://doi.org/10.1117/1.JMI.4.4.043502
- 31. Hagen F, Walder L, Fritz L, et al. Image quality and radiation dose on contrast-enhanced chest CT acquired on a clinical photon-counting detector CT vs. second-generation dual-source CT in an oncologic cohort: preliminary results. *Tomography*. 2022;8(3): 1466-1476. https://doi.org/10.3390/tomography8030119.
- 32. Steinberg J, Siegel MJ, Ramirez-Giraldo JC. Early experience using dual-source photon counting detector CT for pediatric thoracic

- CT examinations: evaluation of radiation dose and acquisition. In: *Proceedings SPR Annual Meeting*, Austin TX, May 16–20, 2023.
- 33. Boccalini S, Si-Mohamed SA, Lacombe H, et al. First in-human results of computed tomography angiography for coronary stent assessment with a spectral photon counting computed tomography. *Invest Radiol.* 2022;57(4):212-221. https://doi.org/10.1097/RLI.0000000000000085
- 34. Euler A, Higashigaito K, Mergen V, et al. High-pitch photon-counting detector computed tomography angiography of the aorta. *Invest Radiol.* 2022;57(2):115-121. https://doi.org/10.1097/RLI.0000000000000816
- 35. Siegel MJ, Bhalla S, Cullinane M. Dual-energy CT material decomposition in pediatric thoracic oncology. *Radiol Imaging Cancer*. 2021;3(1):e200097. https://doi.org/10.1148/rycan.2021200097